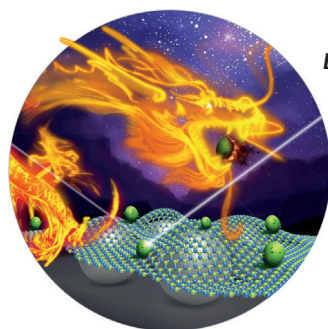
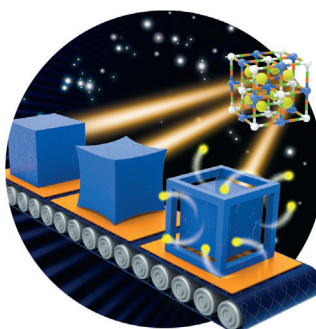


... is described by T. Lectka et al. in their Communication on page 8266 ff. Anchimeric assistance by a C–F bond positioned rigidly over an arene molecule strongly activates the ring toward electrophilic nitration. The lone electron pairs of fluorine effect stabilization of the transition state that leads to the arenium intermediate. In the picture, the C–F bond (human figure above the ice) reaches through the aromatic ring to assist the nitronium figure submerged below.

Hollow Nanostructures

A preferential etching method for synthesizing monocrystalline nanoframes of a Prussian blue analogue is described by M. Hu et al. in their Communication on page 8228 ff. The microfabricated nanoframes are active cathode materials with applicability to alkaline ion batteries.

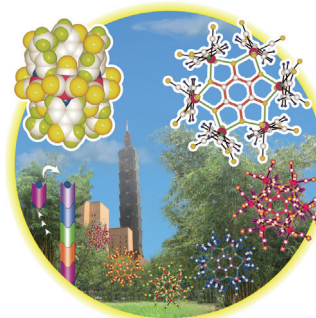


Boron Nitride Nanosheets

In their Communication on page 8405 ff., Y. Chen, L. H. Li, and co-workers show that covering plasmonic silver nanoparticles with atomically thin boron nitride nanosheets greatly enhances the SERS sensitivity.

Supramolecular Chemistry

T. W. Tseng, K. L. Lu, and co-workers show in their Communication on page 8343 ff. how macromolecular building blocks can be stacked together to give dissectible bamboo-like metal-organic tubes.



How to contact us:

Editorial Office:

E-mail: angewandte@wiley-vch.de

Fax: (+49) 62 01–606-331

Telephone: (+49) 62 01–606-315

Reprints, E-Prints, Posters, Calendars:

Carmen Leitner

E-mail: chem-reprints@wiley-vch.de

Fax: (+49) 62 01–606-331

Telephone: (+49) 62 01–606-327

Copyright Permission:

Bettina Loycke

E-mail: rights-and-licences@wiley-vch.de

Fax: (+49) 62 01–606-332

Telephone: (+49) 62 01–606-280

Online Open:

Margitta Schmitt

E-mail: angewandte@wiley-vch.de

Fax: (+49) 62 01–606-331

Telephone: (+49) 62 01–606-315

Subscriptions:

www.wileycustomerhelp.com

Fax: (+49) 62 01–606-184

Telephone: 0800 1800536 (Germany only)
+44(0) 1865476721 (all other countries)

Advertising:

Marion Schulz

E-mail: mschulz@wiley-vch.de

Fax: (+49) 62 01–606-550

Telephone: (+49) 62 01–606-565

Courier Services:

Boschstrasse 12, 69469 Weinheim

Regular Mail:

Postfach 101161, 69451 Weinheim

Angewandte Chemie International Edition is a journal of the Gesellschaft Deutscher Chemiker (GDCh), the largest chemistry-related scientific society in continental Europe. Information on the various activities and services of the GDCh, for example, cheaper subscription to *Angewandte Chemie International Edition*, as well as applications for membership can be found at www.gdch.de or can be requested from GDCh, Postfach 900440, D-60444 Frankfurt am Main, Germany.

GDCh

GESELLSCHAFT
DEUTSCHER CHEMIKER

Get the **Angewandte App**
International Edition



Enjoy Easy Browsing and a New Reading Experience on Your Smartphone or Tablet

- Keep up to date with the latest articles in Early View.
- Download new weekly issues automatically when they are published.
- Read new or favorite articles anytime, anywhere.



Service

Spotlight on Angewandte's Sister Journals

8156–8159

Author Profile



"My favorite author (fiction) is Louis Cha (Jin Yong).

My favorite food is Hunan cuisine ..."

This and more about Xiaoping Zeng can be found on page 8160.

Xiaoping Zeng _____ 8160

News



L. Heinke



S. M. Huber



J. Yuan



F. H. Arnold



R. D. Adams

FCI Dozentenpreis:

L. Heinke, S. M. Huber, J. Yuan — 8161

Millennium Technology Prize:

F. H. Arnold _____ 8161

Florida Award:

R. D. Adams _____ 8161

Reviews

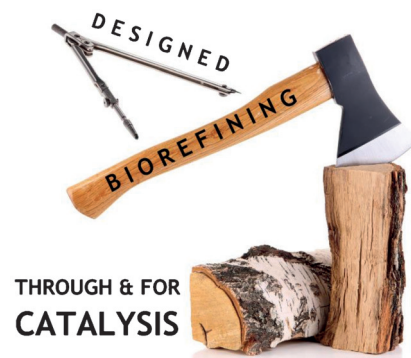
Lignin Valorisation



R. Rinaldi,* R. Jastrzebski, M. T. Clough,
J. Ralph,* M. Kennema,
P. C. A. Bruijninx,*
B. M. Weckhuysen* — 8164–8215

Paving the Way for Lignin Valorisation:
Recent Advances in Bioengineering,
Biorefining and Catalysis

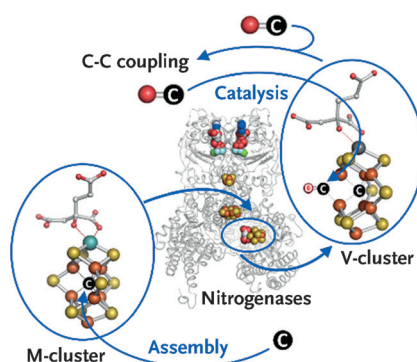
Seeing the wood for the trees: Lignin is an abundant biopolymer with a high carbon content and high aromaticity. A critical analysis of “upstream” and “downstream” elements of lignin valorisation is given, including bioengineering, biorefining, and catalysis.



Nitrogenases

Y. Hu,* M. W. Ribbe* — 8216–8226

Nitrogenases—A Tale of Carbon Atom(s)



A close rapport exists between nitrogenase and carbon through the interstitial carbide of the cofactor of nitrogenase and through the ability of nitrogenase to reduce small carbon compounds to hydrocarbons. Recent advances reveal a radical-SAM-dependent mechanism of carbide insertion into the nitrogenase cofactor and suggest a role of the interstitial carbide in maintaining the stability while permitting certain flexibility of the cofactor structure during catalysis.

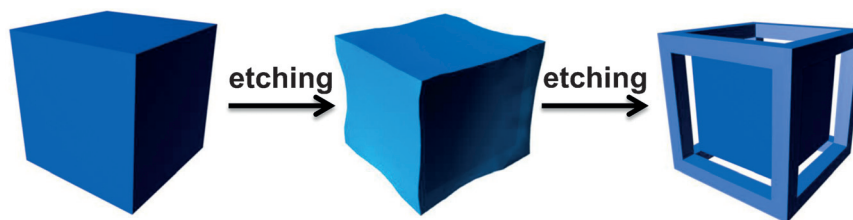
Communications

Cathodic Materials

W. Zhang, Y. Zhao, V. Malgras, Q. Ji,
D. Jiang, R. Qi, K. Ariga, Y. Yamauchi,
J. Liu,* J.-S. Jiang,* M. Hu* — 8228–8234



Synthesis of Monocrystalline Nanoframes
of Prussian Blue Analogues by Controlled
Preferential Etching



A preferential etching method is reported for the synthesis of monocrystalline nanoframes of a Prussian blue analogue, without use of organic additives. The

nanoframes showed remarkable rate performance and cycling stability as a cathode material for alkaline ion batteries.

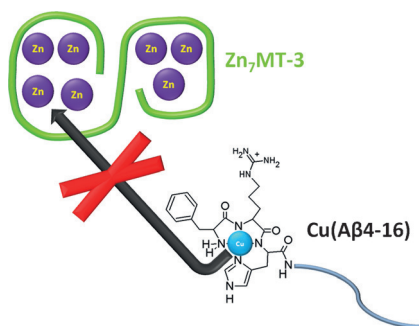
Frontispiece

For the USA and Canada:

ANGEWANDTE CHEMIE International Edition (ISSN 1433-7851) is published weekly by Wiley-VCH, PO Box 101161, 69451 Weinheim, Germany. US mailing agent: SPP, PO Box 437, Emigsville, PA 17318. Periodicals postage

paid at Emigsville, PA. US POSTMASTER: send address changes to *Angewandte Chemie*, John Wiley & Sons Inc., C/O The Sheridan Press, PO Box 465, Hanover, PA 17331. Annual subscription price for institutions: US\$ 16.862/14.051 (valid for print and electronic / print or

electronic delivery); for individuals who are personal members of a national chemical society prices are available on request. Postage and handling charges included. All prices are subject to local VAT/sales tax.

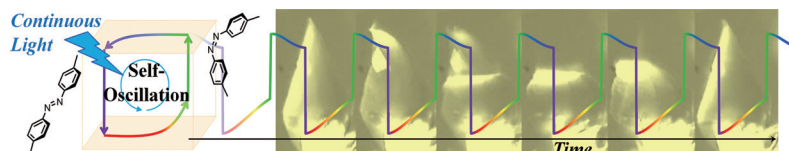


Collecting coppers: Aβ4-42 is a major species of Aβ peptide in the brain and has been demonstrated to bind Cu^{II} with an affinity approximately 3000 times higher than the commonly studied Aβ1-42 and Aβ1-40 peptides. Zinc-bound metallothionein-3 (Zn₇MT-3) is not able to capture copper (blue) from a high-affinity Cu^{II} complex of the model peptide Aβ4-16. This finding supports a role for the Aβ4-42 as a Cu^{II} scavenger in the synaptic cleft.

Amyloid-β Peptides

N. E. Wezrynfeld, E. Stefaniak, K. Stachucy, A. Drozd, D. Płonka, S. C. Drew, A. Krężel, W. Bal* — 8235 – 8238

Resistance of Cu(Aβ4-16) to Copper Capture by Metallothionein-3 Supports a Function for the Aβ4-42 Peptide as a Synaptic Cu^{II} Scavenger



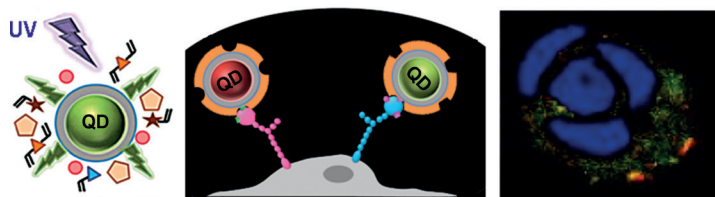
Oscillate wildly: In a limit-cycle self-oscillatory motion of a macroscopic assembly, the assembly permanently flips under continuous blue-light irradiation. Mechanical self-oscillation showing

a spatio-temporal pattern is established by successively alternating photoisomerization processes and multistable phase transitions.

Molecular Motion

T. Ikegami, Y. Kageyama,* K. Obara, S. Takeda* — 8239 – 8243

Dissipative and Autonomous Square-Wave Self-Oscillation of a Macroscopic Hybrid Self-Assembly under Continuous Light Irradiation



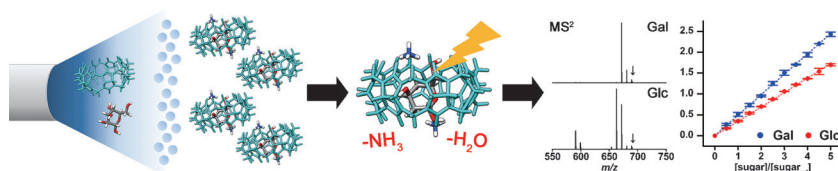
Labels to tell them apart: The visible light emitted from quantum dots excited by UV light was used to photopolymerize a molecularly imprinted polymer (MIP) shell around the QDs. The use of different quantum dots with MIP shells that recognize

glucuronic acid (green) or N-acetylneuraminic acid (red) enabled the multiplexed labeling and imaging of keratinocytes. The labels could be differentiated and quantified on and in the cells.

Bioimaging

M. Panagiotopoulou, Y. Salinas, S. Beyazit, S. Kunath, L. Duma, E. Prost, A. G. Mayes, M. Resmini, B. Tse Sum Bui,* K. Haupt* — 8244 – 8248

Molecularly Imprinted Polymer Coated Quantum Dots for Multiplexed Cell Targeting and Imaging



Mass spectrometry (MS) and phase transfer was used to distinguish between complexes of curcubit[7]uril and four isomeric monosaccharides in the gas phase. The sensitivity of MS enabled

a quantitative analysis of monosaccharide concentrations, and this method could be applied to a variety of other host-guest systems.

Host-Guest Chemistry

H. H. L. Lee, J. W. Lee, Y. Jang, Y. H. Ko, K. Kim,* H. I. Kim* — 8249 – 8253

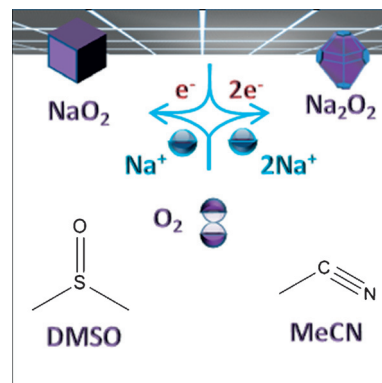
Manifesting Subtle Differences of Neutral Hydrophilic Guest Isomers in a Molecular Container by Phase Transfer



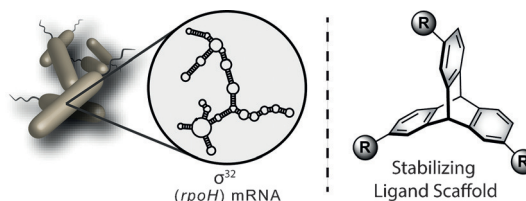
Electrochemistry

I. M. Aldous,
L. J. Hardwick* — 8254–8257Solvent-Mediated Control of the
Electrochemical Discharge Products of
Non-Aqueous Sodium–Oxygen
Electrochemistry

Solvents make the difference: A solvent-dependent mechanism for the oxygen reduction reaction in the presence of sodium is reported. NaO_2 is formed in high donor number solvents, and in low donor number solvents Na_2O_2 formation is observed.



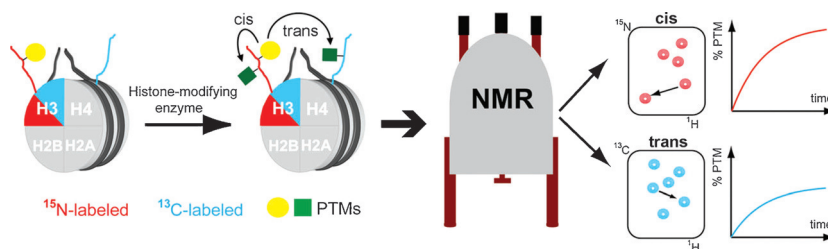
RNA

S. A. Barros, I. Yoon,
D. M. Chenoweth* — 8258–8261Modulation of the *E. coli* *rpoH*
Temperature Sensor with Triptycene-
Based Small Molecules

In *E. coli*, the heat shock response is regulated by an alternative σ factor, σ^{32} , which is encoded by the *rpoH* gene. This

σ^{32} mRNA temperature sensor can be modulated with triptycenes to thermally control gene expression.

Histone Modifications

S. Liokatis,* R. Klingberg, S. Tan,
D. Schwarzer — 8262–8265Differentially Isotope-Labeled
Nucleosomes To Study Asymmetric
Histone Modification Crosstalk by Time-
Resolved NMR Spectroscopy

Telling twins apart: Two copies of a single core histone were subjected to differential isotope-labeling and asymmetric post-translational modification (PTM) and then used to reconstitute nucleosomes. Reaction of these asymmetrically modi-

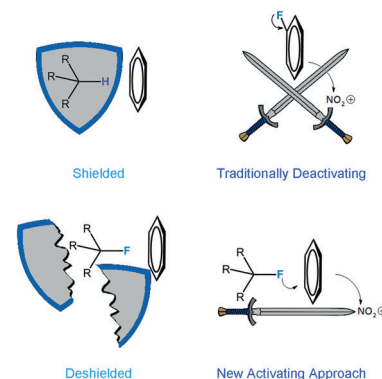
fied nucleosomes with histone-modifying enzymes enabled NMR monitoring of modification crosstalk in cis and in trans, in a time-resolved, qualitative, and quantitative manner.



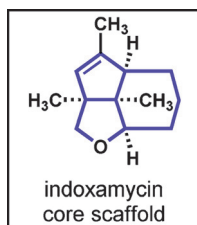
Fluorine Chemistry

M. G. Holl, M. D. Struble, P. Singal,
M. A. Siegler, T. Lectka* — 8266–8269Positioning a Carbon–Fluorine Bond over
the π Cloud of an Aromatic Ring: A
Different Type of Arene Activation

Stabilizing effect of fluorine: A chemical species was synthesized that contained a carbon–fluorine bond positioned tightly over the π cloud of an aromatic ring. This rigid C–F...Ar interaction played a prominent role in both its reaction chemistry and spectroscopy. The results establish fluorine as a through-space directing/activating group that complements the traditional role of fluorine as an overall deactivating aryl substituent.



Front Cover



Methods for functionalizing carbon–hydrogen bonds are featured in a new synthesis of the tricyclic core architecture that characterizes the indoxamycin family of secondary metabolites. A diastereoselective dirhodium carbene insertion followed by an ester-directed oxidative Heck cyclization are key steps of this synthesis.

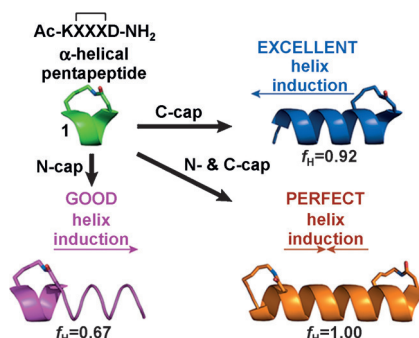
Total Synthesis

T. A. Bedell, G. A. B. Hone, D. Valette, J.-Q. Yu, H. M. L. Davies, E. J. Sorensen* **8270–8274**

Rapid Construction of a Benzo-Fused Indoxamycin Core Enabled by Site-Selective C–H Functionalizations



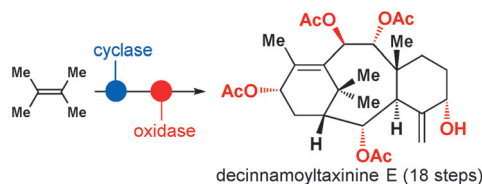
Pep up your peptide: When an α -helical cyclic pentapeptide **1** was appended to one or both ends of a palindromic peptide ARAARAARA ($\leq 5\%$ helicity), 67, 92, or 100% α -helicity of the resulting peptide was observed (see picture). From the C-terminus of peptides, **1** nucleated at least six α -helical turns. Imperfect alignment of a backbone amide in **1** reduced helix nucleation when **1** was attached to the N-terminus, but was corrected by a second unit of **1**.



α -Helical Peptides

H. N. Hoang, R. W. Driver, R. L. Beyer, T. A. Hill, A. D. de Araujo, F. Plisson, R. S. Harrison, L. Goedecke, N. E. Shepherd,* D. P. Fairlie* **8275–8279**

Helix Nucleation by the Smallest Known α -Helix in Water



Take two: Starting from a simple feedstock olefin, highly oxidized natural taxanes were constructed using two-phase terpene synthesis. This work lays the

critical groundwork necessary to access even higher oxidized taxanes in a more practical fashion.

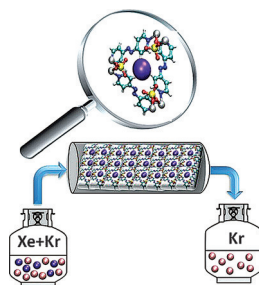
Natural Products

C. Yuan, Y. Jin, N. C. Wilde, P. S. Baran* **8280–8284**

Short, Enantioselective Total Synthesis of Highly Oxidized Taxanes



Try HUMming this: An underexplored class of porous materials called hybrid ultra-microporous materials (HUMs) affords new benchmark selectivity for Xe separation from Xe/Kr mixtures. They have two distinct types of micropores, one of which is lined by CrO_4^{2-} anions. Modeling studies indicate that the selectivity arises from synergy between the pore size and the strong electrostatics afforded by the CrO_4^{2-} anions.



Xenon Sorption

M. H. Mohamed, S. K. Elsaidi, T. Pham, K. A. Forrest, H. T. Schaefer, A. Hogan, L. Wojtas, W. Xu, B. Space, M. J. Zaworotko, P. K. Thallapally* **8285–8289**

Hybrid Ultra-Microporous Materials for Selective Xenon Adsorption and Separation

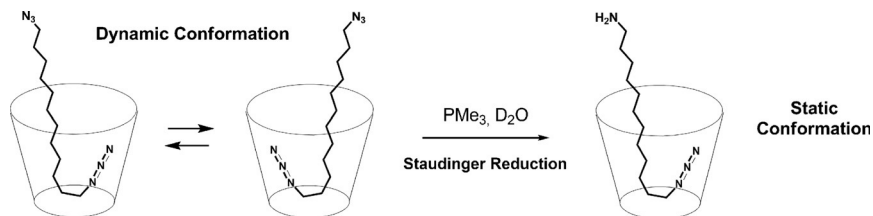


Supramolecular Chemistry

D. Masseroni, S. Mosca, M. P. Mower,
D. G. Blackmond,*
J. Rebek, Jr.* ————— 8290–8293



Cavitands as Reaction Vessels and
Blocking Groups for Selective Reactions in
Water



Reaction shutdown: A deep, water-soluble cavitand allows the selective monoreduction of diazides to monoamines. The unusual reaction pathway can be

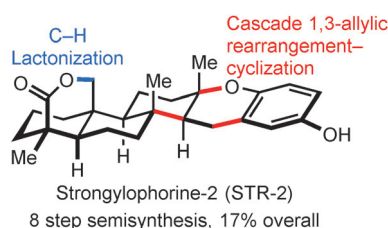
explained by different folding conformations of the starting materials and products inside the container.

Natural Product Synthesis

W. Yu, P. Hjerrild, J. Overgaard,
T. B. Poulsen* ————— 8294–8298



A Concise Route to the Strongylophorines



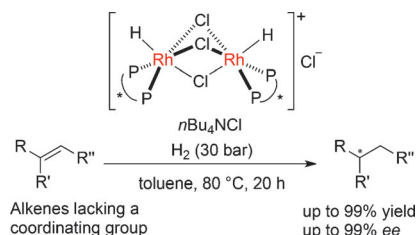
No detours: A powerful semisynthetic strategy to meroterpenoids of the strongylophorine (STR) family is reported. Starting from the abundant sesquiterpene isocupressic acid, a new Lewis acid mediated allylic rearrangement–cyclization cascade and a strategic methyl C–H activation reaction enabled expedient construction of seven members of the STR family, including STR-2.

Asymmetric Hydrogenation

Y. Kita, S. Hida, K. Higashihara, H. S. Jena,
K. Higashida, K. Mashima* — 8299–8303



Chloride-Bridged Dinuclear Rhodium(III)
Complexes Bearing Chiral Diphosphine
Ligands: Catalyst Precursors for
Asymmetric Hydrogenation of Simple
Olefins



Dinuclear rhodium(III) complexes were highly catalytically active for asymmetric hydrogenation of simple olefins in contrast to widely utilized rhodium(I) catalytic systems.

Inside Cover

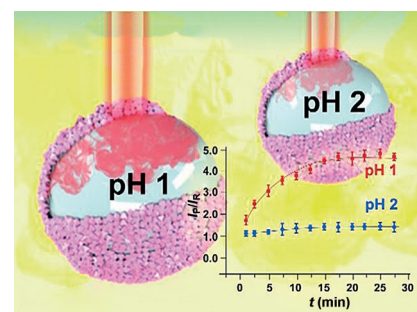
Liquid–Liquid Interfacial Reactors

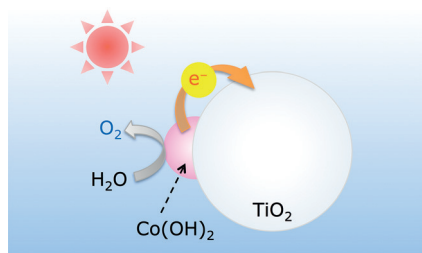
G. C. Phan-Quang, H. K. Lee,
X. Y. Ling* ————— 8304–8308



Isolating Reactions at the Picoliter Scale:
Parallel Control of Reaction Kinetics at the
Liquid–Liquid Interface

Isolation and monitoring of molecules at the picoliter scale: Colloidosomes comprised of silver octahedra assembled at the interface of a water-in-decane emulsion are used as a picoreactor capable of isolating the interfacial protonation of dimethyl yellow. Parallel SERS monitoring of multiple reactions is performed simultaneously, permitting identification of reaction isomers and kinetics.



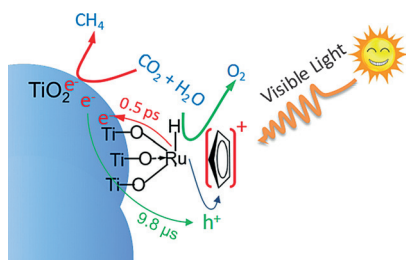


When rutile TiO_2 , a wide-band-gap semiconductor, is modified with cobalt hydroxide nanoclusters, it can be used for photocatalytic water oxidation under visible-light irradiation at wavelengths of up to 850 nm. This material thus constitutes the first particulate photocatalyst that operates at such long wavelengths.

Water Oxidation

K. Maeda,* K. Ishimaki, Y. Tokunaga, D. Lu, M. Eguchi — 8309–8313

Modification of Wide-Band-Gap Oxide Semiconductors with Cobalt Hydroxide Nanoclusters for Visible-Light Water Oxidation



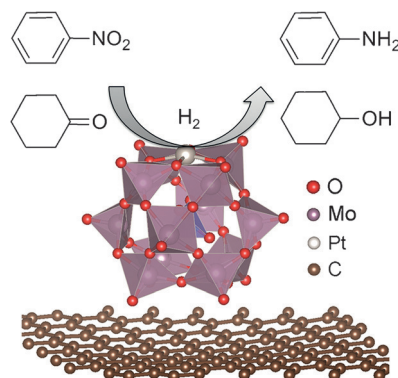
Injector seat: A Ru complex bound to a TiO_2 surface can be locally excited by visible light to rapidly inject electrons into the TiO_2 host, in approximately 0.5 ps. The resulting long-lived charge-separated state with a half-life of 9.8 μs implements the CO_2 -to- CH_4 reduction with H_2O at a quantum yield of 0.56% and almost 100% selectivity.

CO_2 Photoreduction

H. Huang, J. Lin, G. Zhu, Y. Weng, X. Wang, X. Fu, J. Long* — 8314–8318

A Long-Lived Mononuclear Cyclopentadienyl Ruthenium Complex Grafted onto Anatase TiO_2 for Efficient CO_2 Photoreduction

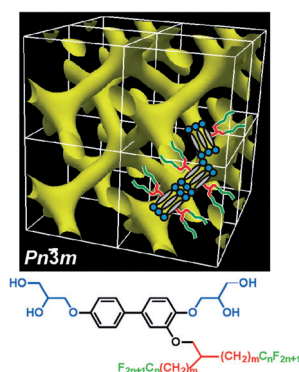
An atomically dispersed Pt_1 catalyst has been developed with a high catalyst loading where each Pt atom is anchored on supported phosphomolybdic acid with distorted square-planar coordination geometry. The catalyst is highly active for nitrobenzene and cyclohexanone hydrogenation.



Single-Atom Catalysts

B. Zhang, H. Asakura, J. Zhang, J. Zhang, S. De, N. Yan* — 8319–8323

Stabilizing a Platinum₁ Single-Atom Catalyst on Supported Phosphomolybdic Acid without Compromising Hydrogenation Activity



Rod-like bolaamphiphiles with branched side chains form the first confirmed thermotropic liquid-crystal cubic phase of the double diamond type. Each segment of the two networks in the structure contains two bundles of biphenyl cores lying along the segment axis. Space-filling geometric calculations are employed to explain why this tightly knit double-network structure with four-way junctions is so rare.

Liquid Crystals

X. B. Zeng, M. Prehm, G. Ungar,* C. Tschierske,* F. Liu* — 8324–8327

Formation of a Double Diamond Cubic Phase by Thermotropic Liquid Crystalline Self-Assembly of Bundled Bolaamphiphiles

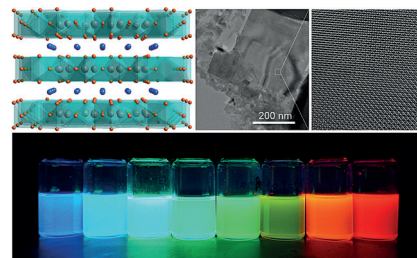
Luminescent Nanoparticles

K.-H. Wang, L. Wu, L. Li, H. B. Yao,*
H. S. Qian, S. H. Yu* — 8328–8332



Large-Scale Synthesis of Highly Luminescent Perovskite-Related CsPb₂Br₅ Nanoplatelets and Their Fast Anion Exchange

The fast and the luminous: A new type of highly luminescent cesium lead halide nanoplatelets show fast anion exchange. Fast anion exchange in the as-synthesized CsPb₂Br₅ nanoplatelets has also been demonstrated to extend their photoluminescence spectra to the entire visible spectral region of 410 nm–670 nm.

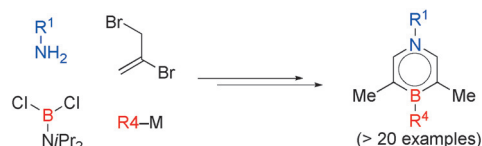


BN heterocycles

X. Liu, Y. Zhang, B. Li, L. N. Zakharov,
M. Vasiliu, D. A. Dixon,*
S.-Y. Liu* — 8333–8337



A Modular Synthetic Approach to Monocyclic 1,4-Azaborines



Now BN done: A simple and general method for the synthesis of a wide range of monocyclic 1,4-azaborines, including the first examples containing B with heteroatom substituents is described. Post-heterocycle-formation olefin isomer-

ization was employed as a key strategy. This new synthetic method provides fundamental insight into the resonance stabilization and photophysical properties of 1,4-azaborines.

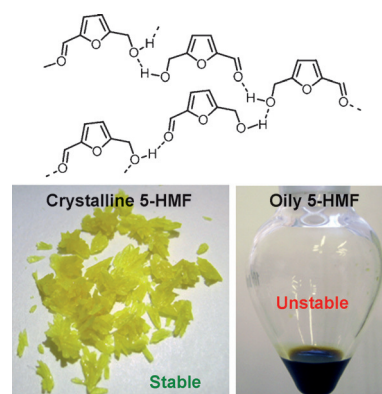
Carbohydrates

K. I. Galkin, E. A. Krivodaeva,
L. V. Romashov, S. S. Zalesskiy,
V. V. Kachala, J. V. Burykina,
V. P. Ananikov* — 8338–8342



Critical Influence of 5-Hydroxymethylfurfural Aging and Decomposition on the Utility of Biomass Conversion in Organic Synthesis

Acting one's age: Aging and decomposition processes of oily 5-hydroxymethylfurfural (5-HMF) were evaluated by spectral studies, which revealed the presence of a specific arrangement of 5-HMF molecules in solution resulting from a hydrogen-bonding network. Blocking the hydrogen-bonding network by a suitable protecting group avoided decomposition during the synthesis and facilitated extraction of the product from the reaction mixture.



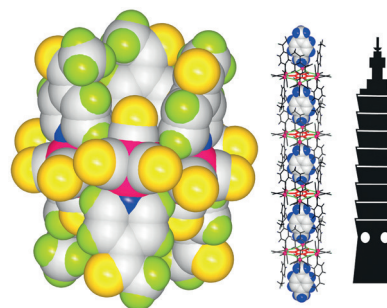
Metal–Organic Nanotubes

T. W. Tseng,* T. T. Luo, S. H. Liao,
K. H. Lu, K. L. Lu* — 8343–8347



Isostructural Synthesis of Dissectible Molecular Bamboo Tubes of Hexarhenium(I) Benzene-1,2,3,4,5,6-hexaolate Complexes

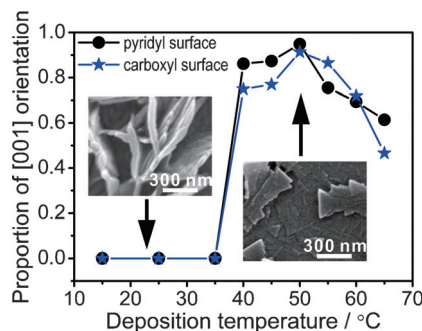
Taipei 101: A family of bamboo-like tubular assemblies consisting of in situ synthesized interlocking macromolecular blocks, which have a doubly tri-legged structure, presents an archetypal approach to the systematic formation of dissectible molecular bamboo tubes (resembling the form of the tower Taipei 101; see picture).



Back Cover



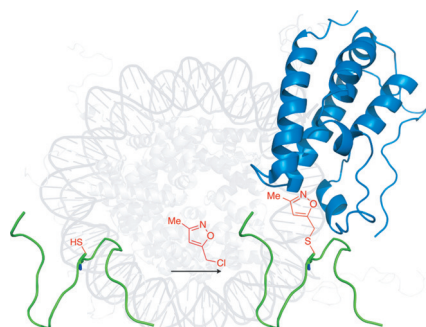
The well-appreciated surface template effects are not sufficient to control surface-attached metal–organic framework growth in systems with low symmetry. Instead, crystal ripening and the trend towards the minimization of surface energies dominate the growth behavior and can be exploited to attain well-oriented crystallites.



Crystal Growth

X. J. Yu, J. L. Zhuang, J. Scherr,
T. Abu-Husein, A. Terfort* — 8348–8352

Minimization of Surface Energies and Ripening Outcompete Template Effects in the Surface Growth of Metal–Organic Frameworks

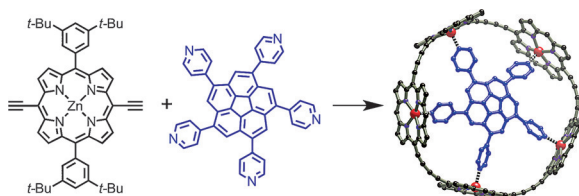


Hang ten: Ten isoxazole-containing amino acids were synthesized, three of which were incorporated into a histone H4-mimicking peptide, and shown to bind to the first bromodomain of BRD4. A complementary tag and modify strategy allows addition of a 3-, 4-, or 5-dimethyl-isoxazole onto the cysteine residues of a histone H4-mimicking peptide, and the full histone H3 protein.

Protein Modifications

A. R. Sekirnik (née Measures),
D. S. Hewings, N. H. Theodoulou,
L. Jursins, K. R. Lewendon, L. E. Jennings,
T. P. C. Rooney, T. D. Heightman,
S. J. Conway* — 8353–8357

Isoxazole-Derived Amino Acids are Bromodomain-Binding Acetyl-Lysine Mimics: Incorporation into Histone H4 Peptides and Histone H3



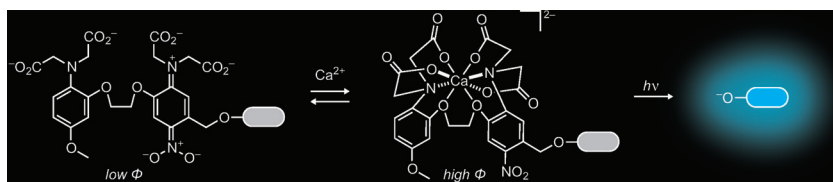
Strained to making point: Two templates were tested for their ability to direct the formation of a π -conjugated cyclic porphyrin pentamer. 1,3,5,7,9-Penta(4-pyridyl)corannulene was found to be more

effective than a ferrocene-based template, despite the fact that the radius of its N5 ligand set is almost 1 Å too small to fit the cavity of the nanoring.

Templated Synthesis

P. Liu, Y. Hisamune, M. D. Peeks,
B. Odell, J. Q. Gong, L. M. Herz,
H. L. Anderson* — 8358–8362

Synthesis of Five-Porphyrin Nanorings by Using Ferrocene and Corannulene Templates



A chemical coincidence detector: The first Ca^{2+} -sensitive photocage, which releases a small molecule only in the presence of both light and elevated Ca^{2+} concentrations, has been synthesized. Caging a

fluorophore with this ion-sensitive moiety yields a system that can permanently mark active neurons during an illumination-defined time period.

Photochemistry

L. M. Heckman, J. B. Grimm,
E. R. Schreiter, C. Kim, M. A. Verdecia,
B. C. Shields, L. D. Lavis* — 8363–8366

Design and Synthesis of a Calcium-Sensitive Photocage



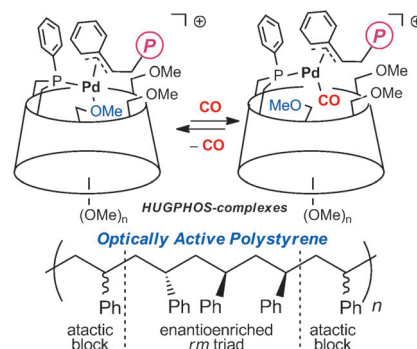
Asymmetric Polymerization

M. Jouffroy, D. Armspach, D. Matt,
K. Osakada, D. Takeuchi* — 8367–8370



Synthesis of Optically Active Polystyrene
Catalyzed by Monophosphine Pd
Complexes

Chain gang: Cationic Pd^{II} monophosphine complexes derived from α - and β -cyclodextrins (CDs) catalyze the homopolymerization of styrene under carbon monoxide pressure. Although CO coordination takes place under catalytic conditions, both complexes catalyze the formation of CO-free styrene polymers (magenta P). These macromolecules display optical activity as a result of the presence of stereoregular sequences within the overall atactic structure.

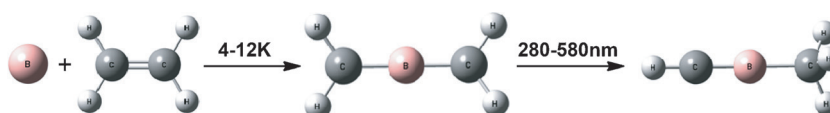


Reaction Mechanisms

J. Jian, H. Lin, M. Luo, M. Chen,
M. Zhou* — 8371–8374



Observation of Spontaneous C=C Bond
Breaking in the Reaction between Atomic
Boron and Ethylene in Solid Neon



C=C bond activation: A ground-state boron atom selectively inserts into the strong C=C bond of ethylene in solid neon to spontaneously form the compound

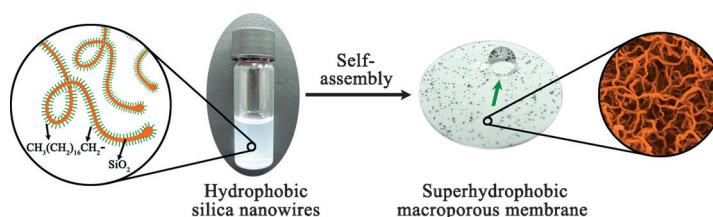
H₂CBCH₂. This compound can further isomerize to the less stable isomer HCBCH₃ under UV light excitation. Atom colors: B = pink; C = gray; H = white.

Membranes

D. L. Yi, C. L. Xu, R. D. Tang, X. H. Zhang,
F. Caruso, Y. J. Wang* — 8375–8380



Synthesis of Discrete Alkyl-Silica Hybrid
Nanowires and Their Assembly into
Nanostructured Superhydrophobic
Membranes



Down to the wire: Discrete alkyl-silica hybrid nanowires surface-capped with a layer of octadecylsilane are synthesized by an anisotropic sol-gel growth method. The alkyl-silica nanowires disperse well in

ethanol and pentanol, and are used as building blocks to construct three-dimensional, superhydrophobic nanowire membranes by a simple vacuum filtration method.

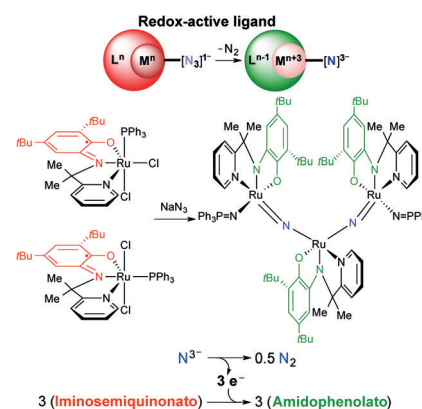
Redox Chemistry

B. Bagh, D. L. J. Broere, M. A. Siegler,
J. I. van der Vlugt* — 8381–8385



Redox-Active-Ligand-Mediated Formation
of an Acyclic Trinuclear Ruthenium
Complex with Bridging Nitrido Ligands

Three strikes aN₂d you're out! The spontaneous azide decomposition on mono-nuclear ruthenium complexes bearing a redox-active aminophenol-derived tridentate NNO ligand selectively generates a rare trinuclear complex with an unsymmetric Ru=N–Ru–N=Ru skeleton, proposedly by oxidative nitride coupling. DFT and experimental data support a pivotal role of the NNO ligand. The bridging bis(nitrido) complex is reactive towards H₂ and hydrogen atom donor species.





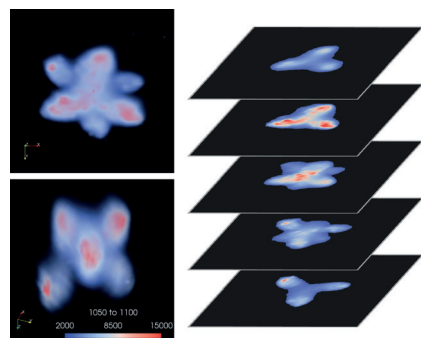
Robust golden architectures: Gold(I) and NaH promote double coupling of isocyanide and propargylamine to give protic $\text{Au}^+/\text{(NHC)}_2$ species, which upon metal-

ation are used in the construction of supramolecular architectures containing a polymeric chain of Cu^I and a nanoscopic piece of cuprite (see scheme).

Supramolecular Chemistry

J. Ruiz,* L. García, D. Sol, M. Vivanco — 8386 – 8390

Template Synthesis, Metalation, and Self-Assembly of Protic Gold(I)/ (NHC)_2 Tectons Driven by Metallophilic Interactions

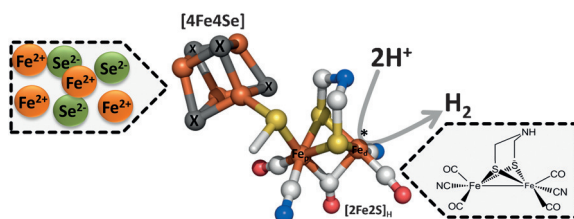


Yes SERS: 3D surface-enhanced Raman scattering (SERS) imaging using highly symmetric chemically synthesized 3D silver microparticles as a SERS substrate was developed. The 3D enhancement patterns of the particles were shown to be very regular and predictable, resembling the particle shape and exhibiting symmetry. This system was applied to the detection of 3D inhomogeneity in a polymer blend, which relies on the predictable enhancement pattern of the substrate.

Raman Spectroscopy

S. Vantasin, W. Ji, Y. Tanaka, Y. Kitahama, M. Wang, K. Wongravee, H. Gatemala, S. Ekgasit, Y. Ozaki* — 8391 – 8395

3D SERS Imaging Using Chemically Synthesized Highly Symmetric Nanoporous Silver Microparticles



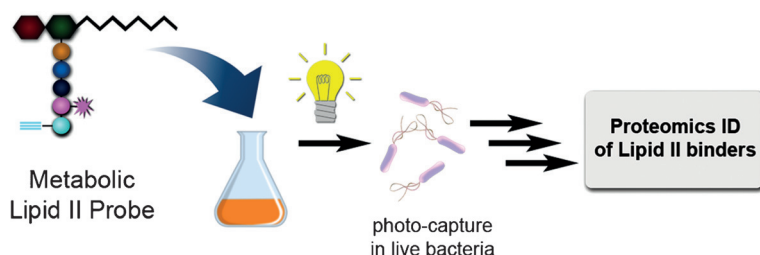
Cofactor swapping: The complex catalytic cofactor of $[\text{FeFe}]$ -hydrogenases (H-cluster) exhibits an unexpected level of compositional plasticity. The complete chemical incorporation of an H-cluster ana-

logue into HYDA1 from *C. reinhardtii* with chalcogenide replacement in the cubane subcluster yields an enzyme variant with full catalytic H_2 -production activity.

Metalloenzymes

J. Noth, J. Esselborn, J. Güldenhaupt, A. Brünje, A. Sawyer, U.-P. Apfel,* K. Gerwert, E. Hofmann, M. Winkler, T. Happe* — 8396 – 8400

$[\text{FeFe}]$ -Hydrogenase with Chalcogenide Substitutions at the H-Cluster Maintains Full H_2 Evolution Activity



Lipid II probes: Lipid II is a critical intermediate in the biosynthesis of bacterial cell walls and it is also the purported target of several antibiotic agents. Unnatural dipeptides were used to gain

entry into the biosynthetic pathway to deliver a dual-functioning probe that can report on potential Lipid II-interacting proteins.

Membrane Probes

S. Sarkar, E. A. Libby, S. E. Pidgeon, J. Dworkin, M. M. Pires* — 8401 – 8404

In Vivo Probe of Lipid II-Interacting Proteins

SERS and Boron Nitride

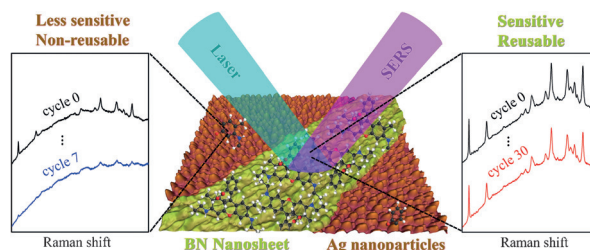
Q. Cai, S. Mateti, W. Yang, R. Jones,
K. Watanabe, T. Taniguchi, S. Huang,
Y. Chen,* L. H. Li* — 8405–8409



Boron Nitride Nanosheets Improve
Sensitivity and Reusability of Surface-
Enhanced Raman Spectroscopy



Inside Back Cover



BN provides silver SERvice: Atomically thin boron nitride (BN) nanosheets coated onto silver nanoparticles improve

the sensitivity, reproducibility, stability, and reusability of surface-enhanced Raman spectroscopy (SERS).

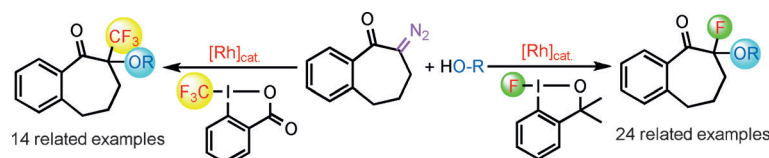
Hypervalent Compounds



W. Yuan, L. Eriksson,
K. J. Szabó* — 8410–8415



Rhodium-Catalyzed Geminal
Oxyfluorination and Oxytrifluoro-
Methylation of Diazocarbonyl
Compounds



All functional: A new reaction for the rhodium-catalyzed geminal-difunctionalization-based fluorination is presented. The substrates are aromatic and aliphatic diazocarbonyl compounds, and the fluo-

rine sources are either benziodoxole or benziodoxolon reagents. A variety of alcohol, phenol, and carboxylic acid reagents were employed to introduce the second functionality.

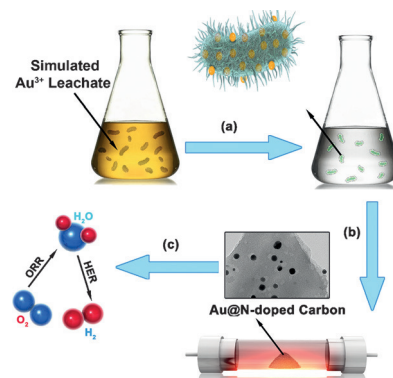
Biological Electrocatalysts

W. Zhou,* T. Xiong, C. Shi, J. Zhou,
K. Zhou, N. Zhu,* L. Li, Z. Tang,
S. Chen — 8416–8420



Bioreduction of Precious Metals by
Microorganism: Efficient Gold@N-Doped
Carbon Electrocatalysts for the Hydrogen
Evolution Reaction

Rags to riches: Gold nanoparticles supported on N-doped carbon (Au@NC) derived from the bioreduction of gold ions by *Pycnoporus sanguineus* cells are active HER electrocatalysts with a small onset potential of -54.1 mV and a Tafel slope of 76.8 mVdec $^{-1}$. The catalyst is a stable and eco-friendly candidate for energy applications. Key: a) bioreduction by Au@microorganism, b) calcination, c) catalysis.

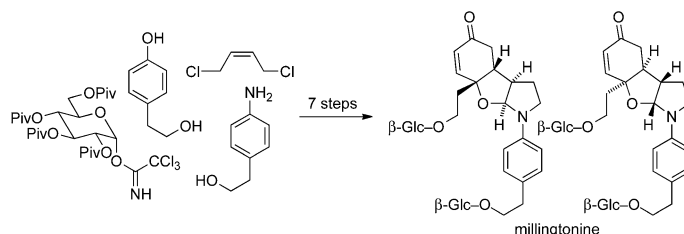


Total Synthesis

P. D. Brown,
A. L. Lawrence* — 8421–8425



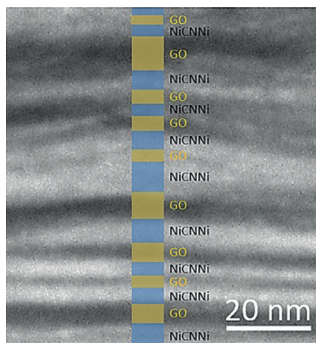
Total Synthesis of Millingtonine



Hidden symmetry: A seven-step total synthesis of the glycosidic alkaloid millingtonine was developed by considering its likely biosynthetic origins. Synthetic results provide evidence in support of

a proposed network of biosynthetic pathways that can account for the formation of several phenylethanoid natural products. Glc = D-glucopyranosyl, Piv = pivaloyl.

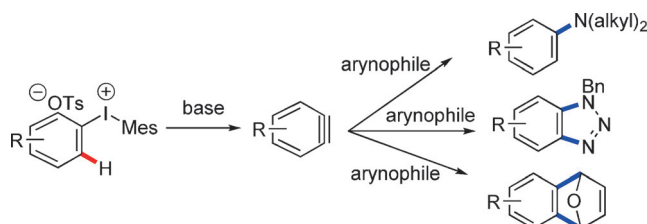
Layer cake: Deposition of nickel-based cyano-bridged coordination polymer (NiCNNi) flakes on the surface of graphene oxide (GO) sheets allows the formation of lamellar nanoarchitectures. Regulated thermal treatment under nitrogen produces an Ni_3C -GO composite with a similar morphology to the starting material. This approach may be applicable to other inorganic-organic hybrids for the formation of ordered layer-by-layer (LbL) architectures.



Nanostructures

M. B. Zakaria, C. Li, Q. Ji, B. Jiang,
S. Tominaka, Y. Ide, J. P. Hill, K. Ariga,*
Y. Yamauchi* **8426–8430**

Self-Construction from 2D to 3D: One-Pot Layer-by-Layer Assembly of Graphene Oxide Sheets Held Together by Coordination Polymers



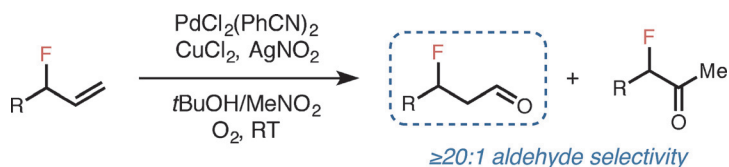
Strategy planning: Unsymmetrical aryl(mesityl)iodonium salts as novel aryne precursors are efficiently prepared in one-pot reactions from aryl iodides and arylboronic acids and facilitate the generation

of elaborate aryne intermediates with high regio- and chemoselectivity. The transient arynes react in cycloaddition reactions with furan and azide and in nucleophilic addition reactions with alicyclic amines.

Arynes

S. K. Sundalam, A. Nilova, T. L. Seidl,
D. R. Stuart* **8431–8434**

A Selective C–H Deprotonation Strategy to Access Functionalized Arynes by Using Hypervalent Iodine



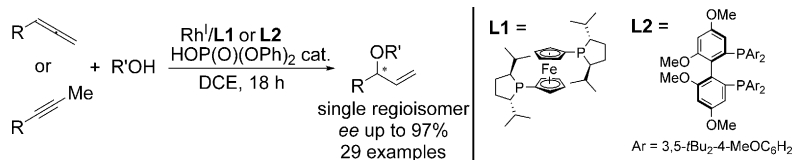
Out of Wack(er): The aldehyde-selective Wacker-type oxidation of allylic fluorides was accomplished using catalytic nitrite, thus providing a direct route to β -fluorinated aldehydes. Allylic fluorides bearing a variety of functional groups are trans-

formed in high yield and regioselectivity. Preliminary mechanistic investigations suggest that inductive effects have a strong influence on the rate and regioselectivity of the oxidation.

Oxidation

C. K. Chu, D. T. Ziegler, B. Carr,
Z. K. Wickens,
R. H. Grubbs* **8435–8439**

Direct Access to β -Fluorinated Aldehydes by Nitrite-Modified Wacker Oxidation



Allenes, alkynes, and alcohols: The rhodium-catalyzed atom-economic coupling of simple and functionalized alcohols with functionalized terminal allenes and inter-

nal alkynes proceeds with chiral bidentate diphosphine ligands and rhodium. The reaction furnishes branched allylic ethers with high regio- and enantioselectivity.

Allylic Compounds

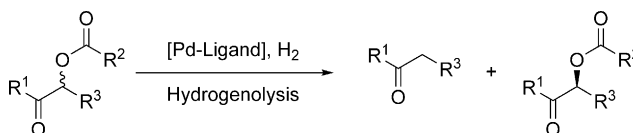
Z. Liu, B. Breit* **8440–8443**

Rhodium-Catalyzed Enantioselective Intermolecular Hydroalkoxylation of Allenes and Alkynes with Alcohols: Synthesis of Branched Allylic Ethers



Kinetic Resolution

J. Chen, Z. Zhang, D. Liu,
W. Zhang* 8444–8447



47 examples, 94–99% yield, 99% ee



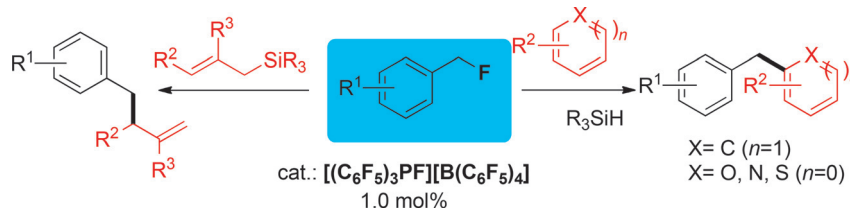
Palladium-Catalyzed Chemo- and Enantioselective C–O Bond Cleavage of α -Acyloxy Ketones by Hydrogenolysis

A break of C–O: A chemoselective C–O bond cleavage of the ester alkyl side chain of α -acyloxy ketones by a palladium-catalyzed hydrogenolysis is reported. Furthermore, an enantioselective C–O bond cleavage was successfully applied to the

kinetic resolution of some acyloins with up to 99% ee. The example ($S/C = 6000$) represents by far the highest catalytic efficiency for a palladium-catalyzed homogeneous hydrogenation.

C–F Activation

J. Zhu, M. Pérez,
D. W. Stephan* 8448–8451

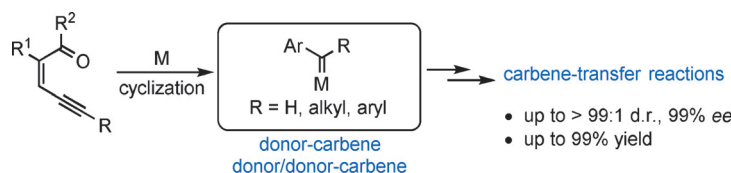


C–F functionalization: Benzyl fluorides are activated by $[(C_6F_5)_3PF][B(C_6F_5)_4]$, affording catalytic routes to 37 1,1-diaryllalkanes

and 14 substituted aryl homoallylic alkenes.

Asymmetric Catalysis

D. Zhu, J. Ma, K. Luo, H. Fu, L. Zhang,*
S. Zhu* 8452–8456



Generous donor: Enantioselective intramolecular C–H insertion and cyclopropanation reactions of donor and donor/donor carbenes by a nondiazo approach are reported. The reactions were con-

ducted in a one-pot manner without slow addition and provided the desired dihydroindole, dihydrobenzofuran, tetrahydrofuran, and tetrahydropyrrole derivatives with up to 99% ee.



Supporting information is available on www.angewandte.org (see article for access details).



A video clip is available as Supporting Information on www.angewandte.org (see article for access details).



This article is available online free of charge (Open Access).



This article is accompanied by a cover picture (front or back cover, and inside or outside).



The Very Important Papers, marked VIP, have been rated unanimously as very important by the referees.



The Hot Papers are articles that the Editors have chosen on the basis of the referee reports to be of particular importance for an intensely studied area of research.